Supporting Information

Tateishi et al. 10.1073/pnas.1315778111

SI Text

Experimental Details for DNP

Fig. S1 is a detailed drawing of the experimental setup. The time sequence of dynamic nuclear polarization (DNP) using photo-excited triplet electrons is shown in Fig. 1*A* in the main text. The laser pulse width and energy were 1 μs and 10 mJ. A microwave pulse with the frequency of 12.05 GHz with the input power of 16 W for pentacene-h_{14} or 10 W for pentacene-d_{14} was applied with the homebuilt cavity. The static magnetic field was set to 0.4 T to irradiate the low field transition of pentacene, $|0\rangle \rightarrow |-1\rangle$ in Fig. 1*A*. Fig. S2 shows the result of finite difference time domain (FDTD) simulation (CST Microwave Studio; AET) of the oscillating field strength in the cavity with the input power of 1 W. From the simulation without the power loss, the oscillating field strengths were estimated to be 1.2 mT for pentacene-h_{14} and 0.96 mT for pentacene-d_{14}. The microwave pulse width was 8 for the samples with pentacene-h_{14} and 20 μs pentacene-d_{14}. The sweep width was ±3.5 mT for pentacene-h_{14} samples and ±2.0 mT for pentacene-d_{14} samples. The sweep shape is shown in Fig. 1*B* in the main text. During the DNP, air was blown onto the sample to prevent the sample heating. ^{1}H NMR was detected with the coil tuned at 17.2 MHz in 0.4 T. Fig. S3 shows ^{1}H NMR signals of thermally polarized ethanol (Fig. S3*A*), *p*-terphenyl-*h*14 doped with pentacene-*h*14(T*h*P*h*) (Fig. S3*B*), and *p*-terphenyl-2′,3′,5′,6′-*d*4 doped with pentacene-*d*14(T*d*P*d*) (Fig. S3*C*). The weights of the single crystal samples were ∼0.6 mg, except for T*h*P*h* (∼0.8 mg). After DNP, we shuttled from the center of the cavity to the center of the NMR coil. Then, the angle between the long molecular axis and the static magnetic field was set to the magic angle. ^{1}H NMR signals were excited with a 3° pulse for hyperpolarized samples to avoid radiation damping and saturation of a low noise amplifier and duplexer. At that sample orientation, the spectra were the narrowest because the dipolar sum was minimum. Ethanol was excited with a 90° pulse. The ESR signals with pentacene-h_{14} and pentacene-d_{14} are shown in Fig. S4. Because, in our setup, both centers of the cavity and the NMR coil were not at the center of the electromagnet, the ESR spectra and the ethanol NMR spectrum were not well resolved due to the static field inhomogeneity.

Polarization Transfer Mechanism

The mechanism of the polarization transfer from the photo-excited triplet electron to nuclear spins is discussed in refs. 1–5. In refs. 2 and 3, the polarization transfer mechanism on nuclear orientation via electron locking (NOVEL) is explained in a study using deuterated and undeuterated triplet molecules and host molecules. In refs. 1, 4, and 5, the polarization transfer mechanism on the integrated solid effect (ISE) is also explained in a study using deuterated and undeuterated pentacene and naphthalene. The detailed study on the polarization transfer in ISE with the sample of *p*-terphenyl doped with pentacene should be included in future work.

Here we briefly review the mechanism of ISE in refs. 1 and 4. In ISE, the field sweep and microwave irradiation near the transition frequency between the triplet sublevels are simultaneously applied. The electron spin resonance spectrum is inhomogeneously broadened by Fermi contact interaction with nuclear spins in the vicinity. The inhomogeneously broadened electron spin packets are adiabatically swept over, and the spin state is locked along the effective field composed of the microwave field and the inhomogeneous field. The Hartmann–Hahn condition between the effective nutation frequency of the electron spins in the rotating frame and the ^{1}H spin Larmor frequency is satisfied at some point of the adiabatic process, where the polarization transfer between electron spins and nuclear spins occurs like conventional cross polarization. In the sample with deuterated pentacene, the polarization is directly transferred to nuclear spins in host molecules.

Field Cycling Experiment

The ^{1}H spin polarization was also determined from the ratio of the asymmetric spectrum of ^{13}C spin (6–8). The experimental setup and the NMR sequence are shown in Fig. S5. The sample pathway to shuttle was in the leakage fields of the superconducting magnet and the electromagnet and the minimum strength was larger than 300 G. Even at 300 G, state mixing between different species (^{1}H, ^{2}H, and ^{13}C) is negligible because the flip-flop terms of the dipolar interactions <30 kHz are averaged out by the much larger Zeeman energy differences >900 kHz. In addition, the ^{1}H T_1 is longer than 1 min even at 300 G and longer than 10 min at 0.4 T and 11.7 T. Therefore, the ^{1}H spin polarization is not decreased during the sample shuttle within 10 s, as was verified in our past study (9). The sample was transferred into the homebuilt solid-state NMR probe (tuned at 125 MHz for ^{13}C spins and 500 MHz for ^{1}H spins) in 11.7 T as the long molecular axis of *p*-terphenyl was set parallel to the field. From the crystal structure studied with X-ray and neutron diffraction (10), the distance between ^{13}C and ^{1}H spins is known to be 1.08 Å. In the orientation, the strength of the dipolar interaction between ^{13}C and ^{1}H spins becomes maximum (20 kHz) at the edges (indicated in Fig. 3 in the main text) and very weak (2.5 kHz) at the other positions. With adequate contact time for cross polarization (CP) between ^{13}C and ^{1}H spins (20 μs), the naturally abundant ^{13}C spin at the edge of the molecule is polarized whereas the other ^{13}C spins are less polarized. After CP, both the ^{1}H and ^{13}C spins flipped back to the static magnetic field. Then, the ^{1}H spin polarization coupled to the ^{13}C spins was recovered due to spin diffusion. Finally, the ^{13}C signal was detected with spin echo. The spectral split width is ∼40 kHz, and therefore the signal comes from the ^{13}C spin at the edge of *p*-terphenyl. The J coupling strength between ^{13}C and ^{1}H spins in benzene rings is less than 100 Hz, and therefore it is much smaller than the dipolar coupling. The polarization was determined by

$$P = \frac{S_{|\uparrow\rangle} - S_{|\downarrow\rangle}}{S_{|\uparrow\rangle} + S_{|\downarrow\rangle}}, \qquad \text{[S1]}$$

where $S_{|\uparrow\rangle}$ and $S_{|\downarrow\rangle}$ are the signal intensities of the right and left peaks.

Synthesis of *p*-Terphenyl-2′,3′,5′,6′-d_4

^{1}H NMR spectra were recorded at 500 MHz with a $CDCl_3$ solvent and $(CH_3)_4Si$ as an internal standard. Electron ionization (EI) mass spectra were recorded at 70 eV. Melting points were measured with a hot-stage apparatus without correction. Elemental analysis was performed at the Graduate School of Science, Osaka University. The R_f value on thin layer chromatography (TLC) was recorded on E. Merck precoated (0.25 mm) silica gel 60 F_{254} plates. Tetrahydrofuran (THF) (dehydrated, stabilizer-free grade) was purchased from Kanto Chemical Co. and further purified by a solvent purification system (MBRAUN-SPS Compact) before use. 1,4-Diiodobenzene-2,3,5,6-d_4 was prepared using commercially available benzene-d_6 (Aldrich) according to ref. 11.

As shown in Fig. S6, 1,4-diiodobenzene-2,3,5,6-d_4 (3.9 g, 11.7 mmol), phenylboronic acid pinacol ester (4.8 g, 23.3 mmol), and silver carbonate (3.9 g, 23.3 mmol) were placed in a 100-mL Schlenk tube. THF (30 mL) was added to the tube and deoxygenated by argon bubbling for 30 min. Tetrakis(triphenylphosphine)palladium (674 mg, 0.583 mmol) was added to the mixture and stirred at 65 °C in an argon atmosphere overnight. The reaction mixture was cooled to room temperature and the colorless precipitate was dissolved with CH_2Cl_2 (250 mL). The resulting solid was filtered, and the filtrate was concentrated under reduced pressure. The residue was completely dissolved with benzene (40 mL) at 70 °C in a hot water bath. After addition of hexane (20 mL), the precipitate was separated by filtration, and the *p*-terphenyl derivative (2.0 g) was obtained as a colorless powder. The powder was further purified by sublimation at 100 °C in vacuo, to give a pure material (1.8 g, 66%) in the form of colorless crystals. M.p. 212–214 °C; $R_f = 0.68$ (5:1 hexane/ethyl acetate); ^{1}H NMR (500 MHz, $CDCl_3$): $\delta = 7.36$ (*t*, $J = 7.4$ Hz, 2H), 7.44–7.48 (m, 4H), 7.64–7.66 ppm (m, 4H); MS (EI): *m/z* (%): 234 (100) M+; elemental analysis calcd (%) for $C_{18}H_{10}D_4$: C, 92.28; H, 4.30; D, 3.42; N, 0.00. Found: C, 92.08; H, 4.14; D, 3.31; N, 0.00.

1. Henstra A, Lin T-S, Schmidt J, Wenckebach WTh (1990) High dynamic nuclear-polarization at room-temperature. *Chem Phys Lett* 165(1):6–10.
2. van den Heuvel DJ, Schmidt J, Wenckebach WTh (1994) Polarizing proton spins by electron-spin locking of photo-excited triplet state molecules. *Chem Phys* 187: 365–372.
3. Henstra A, Wenckebach WTh (2008) The theory of nuclear orientation via electron spin locking (NOVEL). *Mol Phys* 106:859–871.
4. Takeda K (2009) *Triplet State Dynamic Nuclear Polarization* (VDM, Saarbrücken, Germany).
5. Takeda K (2003) Studies on dynamic nuclear polarization using photo-excited triplet electron spins. PhD thesis (Kyoto Univ, Kyoto).
6. Abragam A, Goldman M (1982) *Nuclear Magnetism: Order and Disorder* (Clarendon, Oxford).
7. Waugh JS, Gonen O, Kuhns P (1987) Fourier transform NMR at low temperatures. *J Chem Phys* 86:3816–3818.
8. Morley GW, et al. (2007) Efficient dynamic nuclear polarization at high magnetic fields. *Phys Rev Lett* 98(22):220501.
9. Kagawa A, Negoro M, Takeda K, Kitagawa M (2009) Magnetic-field cycling instrumentation for dynamic nuclear polarization-nuclear magnetic resonance using photoexcited triplets. *Rev Sci Instrum* 80(4):044705.
10. Rietveld HM, Maslen EN, Clews CJB (1970) An X-ray and neutron diffraction refinement of the structure of p-terphenyl. *Acta Crystallogr* 26:693–706.
11. Lulinski P, Skulski L (2000) Iodination of both deactivated and activated arenes with sodium periodate or sodium iodate as the oxidants. *Bull Chem Soc Jpn* 73:951–956.

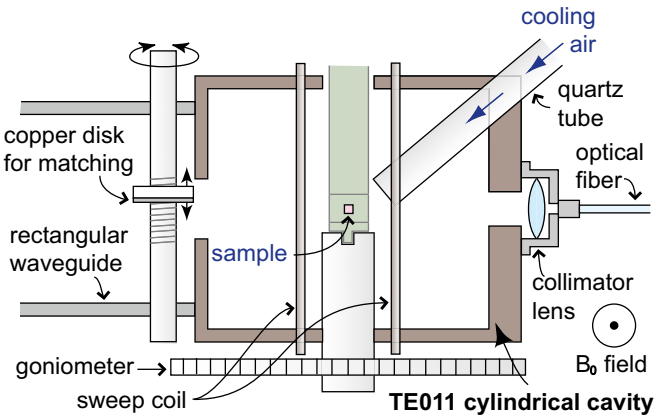

Fig. S1. Detailed drawing of the experimental setup.

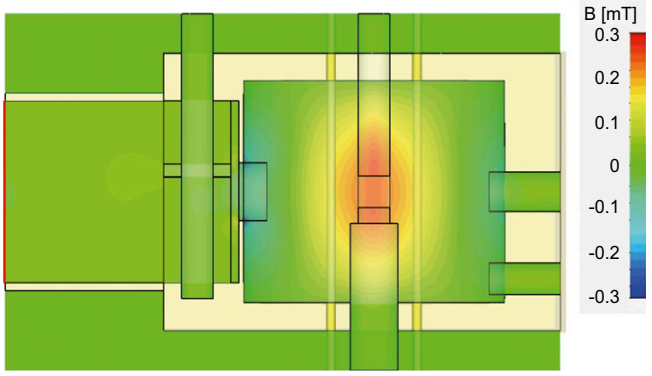

Fig. S2. Simulation result of the oscillating field strength in the cavity.

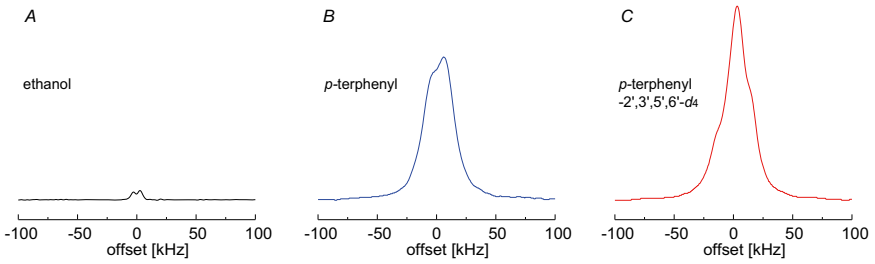

Fig. S3. (*A*–*C*) ^{1}H NMR signals of thermally polarized ethanol (*A*) and T*h*P*h* (*B*) and T*d*P*d* (*C*) after polarization saturated by DNP.

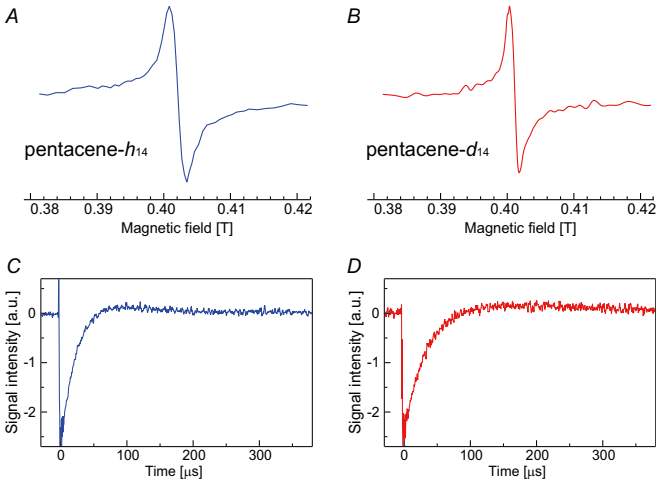

Fig. S4. (*A*–*D*) The ESR spectra of pentacene-h_{14} (*A*) and pentacene-d_{14} (*B*) and the time-domain ESR signals of pentacene-h_{14} (*C*) and pentacene-d_{14} (*D*).

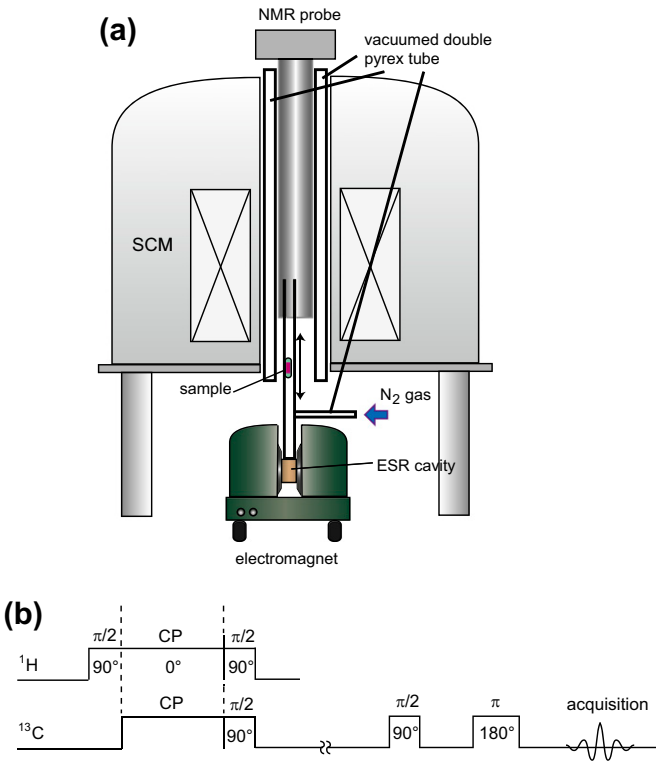

Fig. S5. Experimental setup and NMR pulse sequence for determining polarization from the asymmetric spectrum. (*A*) A schematic image of the experimental setup. (*B*) The sequence for determining polarization from asymmetry.

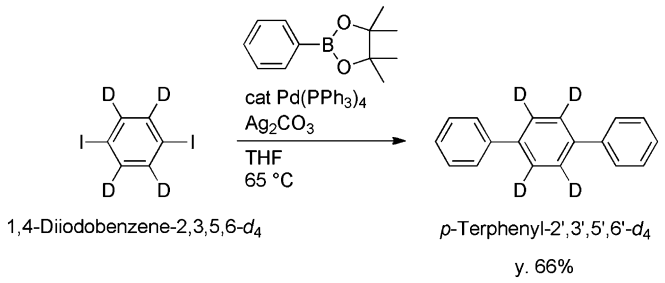

Fig. S6. Synthesis of *p*-terphenyl-2′,3′,5′,6′-d_4.